AIP | Applied Physics Letters

Three-dimensional photonic-crystal emitter for thermal photovoltaic power generation

S. Y. Lin, J. Moreno, and J. G. Fleming

Citation: Appl. Phys. Lett. **83**, 380 (2003); doi: 10.1063/1.1592614
View online: http://dx.doi.org/10.1063/1.1592614
View Table of Contents: http://apl.aip.org/resource/1/APPLAB/v83/i2
Published by the American Institute of Physics.

Related Articles

Correlation between interface energetics and open circuit voltage in organic photovoltaic cells
Appl. Phys. Lett. 101, 233301 (2012)

Correlation between interface energetics and open circuit voltage in organic photovoltaic cells
APL: Org. Electron. Photonics 5, 259 (2012)

New method to assess the loss parameters of the photovoltaic modules
J. Renewable Sustainable Energy 4, 063115 (2012)

Electric double layers allow for opaque electrodes in high performance organic optoelectronic devices
APL: Org. Electron. Photonics 5, 236 (2012)

Electric double layers allow for opaque electrodes in high performance organic optoelectronic devices
Appl. Phys. Lett. 101, 173302 (2012)

Additional information on Appl. Phys. Lett.

Journal Homepage: http://apl.aip.org/
Journal Information: http://apl.aip.org/about/about_the_journal
Top downloads: http://apl.aip.org/features/most_downloaded
Information for Authors: http://apl.aip.org/authors

ADVERTISEMENT

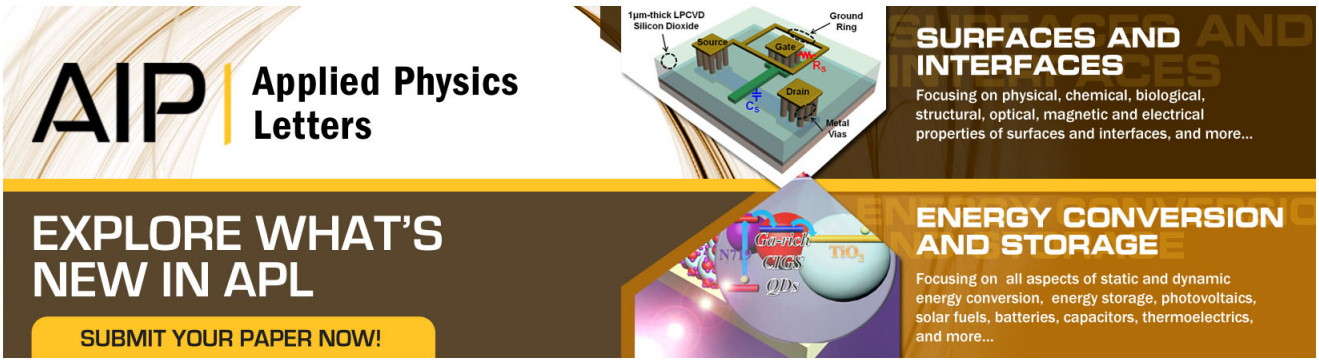

Three-dimensional photonic-crystal emitter for thermal photovoltaic power generation

S. Y. Lin,[a] J. Moreno, and J. G. Fleming
MS 0603, Sandia National Laboratories, P.O. Box 5800, Albuquerque, New Mexico 87185

(Received 7 April 2003; accepted 23 May 2003)

A three-dimensional tungsten photonic crystal is experimentally realized with a complete photonic band gap at wavelengths $\lambda \geqslant 3$ μm. At an effective temperature of $\langle T \rangle \sim 1535$ K, the photonic crystal exhibits a sharp emission at $\lambda \sim 1.5$ μm and is promising for thermal photovoltaic (TPV) power generation. Based on the spectral radiance, a proper length scaling and a planar TPV model calculation, an optical-to-electric conversion efficiency of ~34% and electrical power of ~14 W/cm^2 is theoretically possible. © *2003 American Institute of Physics.*
[DOI: 10.1063/1.1592614]

There is an emerging interest in using thermal photovoltaic (TPV) cells for electric-power generation.[1,2] Similar to a solar cell, in which solar radiation is converted into electricity, a TPV cell converts thermal radiation into electricity. The optical-to-electricity conversion is based on photocurrent generation by those photons having energy exceeding the electronic band gap, ($\hbar\omega_{\text{radiation}} \geqslant E_g$). The portion of photons with $\hbar\omega_{\text{radiation}} \leqslant E_g$ is not useful, leading to a lower conversion efficiency. In other words, E_g is the cutoff energy, below which radiation energy is wasted. To maximize conversion efficiency, it is desirable to have a narrow-band spectrum with its radiation energy slightly above the electronic band gap. While the solar spectrum is given, a thermal radiation spectrum may be modified by choice of radiator materials,[2] by surface structuring[3,4] and also by photonic band gap engineering.[5–9] In particular, a three-dimensional (3D) complete photonic band gap can be used to suppress radiation below the electronic band gap.[7,8] Meanwhile, emission can be enhanced at a narrow band near a photonic band edge or a narrow allowed band.[7,8] If both effects are combined, a nearly ideal radiation spectrum can be obtained.

In this letter, a tungsten 3D photonic crystal is experimentally realized with a complete photonic band gap at wavelengths $\lambda \geqslant 3$ μm. At a sample temperature of ~1535 K, the photonic-crystal emission is suppressed in the photonic band gap regime ($\lambda > 3$ μm), exhibits a peak at $\lambda \sim 1.5$ μm, and a narrow spectral width of $\Delta\lambda \sim 0.9$ μm. This nearly ideal radiation spectrum could lead to an optical-to-electric conversion efficiency of $\eta \sim 34\%$ and electric power density of $p \sim 14$ W/cm^2.

The 3D tungsten photonic crystal is fabricated using a modified silicon process. In the first step, a layer of silicon dioxide is deposited, patterned, and etched to create a mold. The mold is then filled with a 500-nm-thick tungsten film and planarized using a chemical mechanical polishing process. The process is repeated several times. At the end of the process, the silicon dioxide is released from the substrate and the sample is a freely standing thin film. A scanning electron micrograph (SEM) image of the fabricated sample is shown in Fig. 1(a). The one-dimensional (1D) rods represent the shortest $\langle 110 \rangle$ chain of atoms in a diamond lattice.[10,11] The rod-to-rod spacing is $a = 1.5$ μm, the rod width is $w = 0.5$ μm, and rod height $h \sim 0.75$ μm.

In Fig. 1(b), the computed absorption spectrum for an eight-layer photonic-crystal sample is shown. The absorptance is low for $\lambda > 3$ μm (the photonic band gap) and increases slightly at $\lambda \sim 3$–4 μm due to a higher tungsten material absorption at these wavelengths.[12] This band gap has been shown to be a complete band gap, capable of trapping light fully in all three dimensions and for both polarizations.[7] Beyond the photonic band gap regime, there are two strong absorptions. One is at $\lambda = 2.5$ μm with an absorptance of ~40% and the other at $\lambda = 1.5$–1.9 μm with an even stronger absorptance of ~80%. The high absorptance is due to a combination of finite tungsten absorption and a high density of

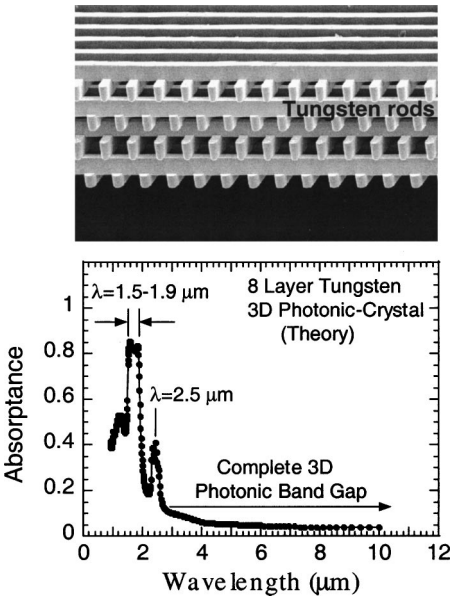

FIG. 1. (a) A SEM view of a 3D tungsten photonic crystal. Within each layer, the 1D rod width is 0.5 μm and the rod-to-rod spacing is 1.5 μm. (b) A computed absorption spectra for an eight-layer 3D tungsten photonic-crystal sample. The absorptance is low for $\lambda > 3$ μm (the photonic band gap), exhibits a peak of ~40% at $\lambda \sim 2.5$ μm, and a high plateau of ~80% at $\lambda \sim 1.5$–1.9 μm.

[a]Electronic mail: slin@sandia.gov

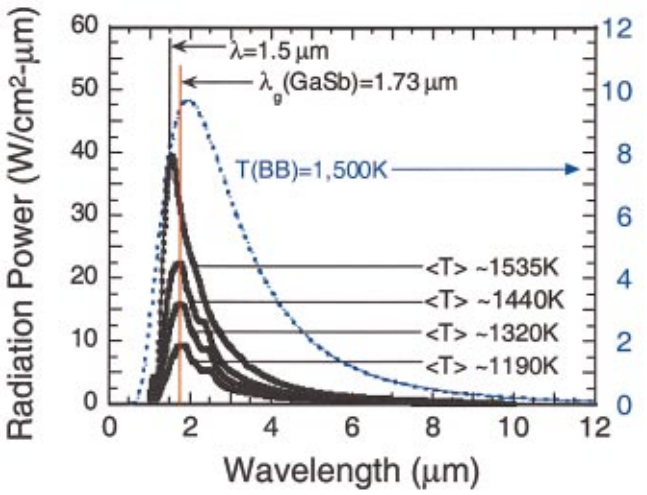

FIG. 2. (Color) The measured photonic-crystal emission power at a bias of $V=3$, 4, 5, and 6.5 V, respectively. The effective temperature, average over the entire sample, is $\langle T\rangle \sim 1190$, 1320, 1440, and 1535 K, respectively. At $\langle T\rangle \sim 1535$ K, the emission peaks at $\lambda \sim 1.5$ μm and has a full width at half maximum of 0.9 μm. The dashed blue line is a blackbody radiation curve. The electronic band gap wavelength of GaSb is also shown as a red line.

photon-states $D(\omega)$ at a narrow band.[13–15] As absorption and emission processes have the same physical origin,[16] a strong narrow absorption is suggestive of a narrow band emission from a photonic-crystal sample.

To achieve emission, the sample is biased by applying a voltage across the photonic-crystal sample and is heated through Joule heating. The emission spectra of the 3D photonic crystal are taken using a standard Fourier-transform infrared spectrometer from $\lambda=1$–15 μm.[17,18] As the sample is operated at high temperatures, it is mounted to be thermally and electrically isolated from its surroundings. To minimize thermal loss, the sample is placed in a vacuum chamber pumped to $\sim 10^{-5}$ Torr. For power density measurements, a commercially available Gentec power meter, calibrated to better than 5%, is used.

In Fig. 2, emission spectra taken at a bias of $V=3$, 4, 5, and 6.5 V are shown, respectively. The effective temperature, averaged over the entire sample, is $\langle T\rangle = 1190$, 1320, 1440, and 1535 K, respectively. It is determined by measuring sample resistivity and by comparing it to the calibrated, temperature-dependent tungsten resistivity. At $V=3$ V, or $\langle T\rangle \sim 1190$ K, the emission consists of a weak peak at $\lambda \sim 2.5$ μm and a stronger peak at $\lambda \sim 1.8$ μm. At a higher temperature, $\langle T\rangle \sim 1535$ K, the stronger peak dominates the spectrum and shifts to $\lambda \sim 1.5$ μm. The dashed blue curve is a blackbody cavity-radiation spectrum, having a peak power density of 9.8 W/cm^2 at $\lambda \sim 2$ μm and a full width at half maximum of $\Delta\lambda(\mathrm{FWHM}) \sim 2.3$ μm. Yet, the photonic-crystal (PBG) emission exhibits a peak power density of 40.5 W/cm^2 at $\lambda \sim 1.5$ μm and a much narrower $\Delta\lambda(\mathrm{FWHM}) \sim 0.9$ μm. To achieve a spectral linewidth this narrow, one would have to heat a blackbody to a temperature of $T \sim 4000$ K. The narrow PBG emission implies a better match of the emission spectrum to electronic band gap of a photovoltaic cell. The higher PBG-emission power than that of a blackbody (BB) emission at a selective wavelength range is beyond the scope of this letter, and is discussed in a separate publication.[8] For reference purposes, the band gap wavelength, $\lambda_{\text{band gap}} \approx 1.73$ μm, of a GaSb photovoltaic cell is shown as a solid red line.

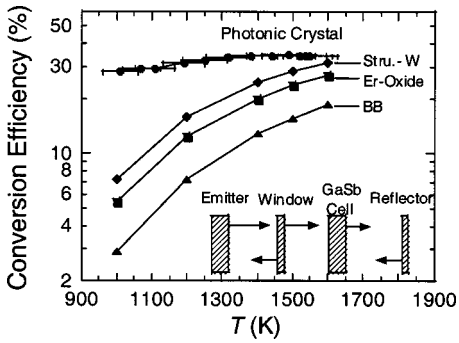

FIG. 3. The computed thermal photovoltaic conversion efficiency for four different emitters at temperatures $T=1000$–1600 K. The PBG emitter has a high efficiency of $\eta=27\%$–33%. In the inset, an illustration of radiative flux in a simple one-dimensional thermal photovoltaic model is shown.

To model photovoltaic energy conversion, a planar system is used to describe radiation heat transfer. This model is intended to evaluate radiator performance and does not include a process to heat the radiator. The radiation model we used is similar to Zenker *et al.*[2] As shown in the inset of Fig. 3, the system consists of an emitter, a cell window (model cell front surface), a GaSb photovoltaic cell, and a reflector. Both an ideal and a realistic window reflectivity are considered.[2] As our photonic-crystal itself emits a spectrally narrow radiation, no filter is used. The GaSb cell is modeled in the context of its thermodynamic limit at $T=300$ K. In this limit, the GaSb internal quantum efficiency is assumed to be one for $\hbar\omega_{\text{radiation}} \geqslant E_g$. It is also assumed that the only loss mechanism in the cell is radiative recombination. The conservation relations between the spectral radiant fluxes are written and symbolically solved using MathCad software. To check our model against Zenker's, the same cases were run for the thermodynamic limit and for an ideal window reflectivity.

In Table I, the model results are shown for three conventional radiators heated to $T=1500$ K. The BB cavity radiator is a broadband emitter and the Er_2O_3 and the structured tungsten radiators are selective emitters.[2] The optical-to-electric efficiency $\eta(\%)$ is defined as: $\eta \equiv p/Q_{\text{radiation}}$, where p is the electric power density in W/cm^2 and $Q_{\text{radiation}}$ is the total radiation power density. Making allowance for the uncertainties in digitizing the window reflectance in Zenker *et al.*, the agreement for all three emitters is quite reasonable.

Using the same model, the potential performance of a photonic-crystal (PBG) emitter is evaluated. To obtain a more optimal performance, the emission wavelength is scaled by 30%. This scaling corresponds to a photonic crys-

TABLE I. A summary of computed efficiency and power for a broadband emitter (the blackbody) and two selective emitters (the Er_2O_3 and the structured tungsten emitters).

	Zenker *et al.*		This work	
Emitter type	η (%)	El. power (W/cm^2)	η (%)	El. power (W/cm^2)
Blackbody	11	3.0	11	3.0
Er_2O_3	26	1.1	24	1.1
Struc.-tungsten	30	1.6	29	1.6

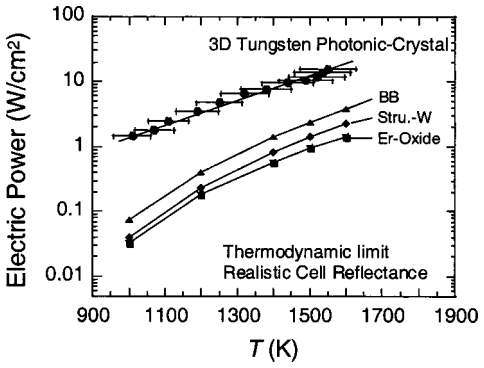

FIG. 4. The computed electric power density for four different emitters at temperatures $T=1000-1600$ K. Photonic-crystal emitter generates the highest output electric power density, yet the structured tungsten and the Er_2O_3 yield the least.

tal with a lattice constant of $a=1.05$ μm. In this analysis, a realistic window reflectivity is used. In Fig. 3, the computed efficiency for the PBG emitter and the three conventional emitters is shown. The PBG emitter has a high efficiency of $\eta=27\%-33\%$ over the entire temperature range. As the peak PBG-emission wavelength does not shift significantly with temperature (see Fig. 2), this nearly constant efficiency is expected. By contrast, the efficiency of the three conventional emitters exhibits a strong temperature dependence. The efficiency of the blackbody emitter increases from 3% to 15% for $T=1000-1600$ K. The efficiency is low as only a small fraction of the blackbody radiation satisfies the cutoff condition: $\hbar\omega_{\text{radiation}} \geqslant E_g$, or $\lambda_{\text{radiation}} \leqslant \lambda_{\text{band gap}}=1.73$ μm. For $T=1000-1600$ K, a blackbody emission peaks at λ_{peak} (μm)$\cong 2898/T(\text{K})=1.81-2.89$ μm>1.73 μm. Efficiency of the selective emitters, both Er_2O_3 and structured tungsten, is higher than that of a blackbody emitter. This is due to their shorter peak emission wavelength $\lambda_{\text{peak}} \approx 1.55-1.7$ μm and narrower spectral width[2,3] compared with that of a blackbody emitter.

In Fig. 4, the computed power density is plotted as a function of temperature for the PBG emitter and the three conventional emitters. As temperature is increased, radiation energy density is increased accordingly, leading to higher power density for all four emitters. The highest electric power density is generated by the PBG emitter. At $\langle T\rangle=1500$ K, the expected electric power is $p=13$, 2.4, 1.4, and 0.94 W/cm^2 for PBG, BB, structured tungsten, and Er_2O_3 emitters, respectively. This high value of electric power from a PBG emitter is a result of a narrow spectral width and high optical power density as shown in Fig. 2. The structured tungsten and Er_2O_3 produce the least electric power. This is because, for these selective emitters, their total radiation intensity for $\hbar\omega_{\text{radiation}} \geqslant E_g$ is less than that of a blackbody emitter. A selective emitter can yield high conversion efficiency, but often at the expense of a lower electric power density.

In summary, a 3D tungsten photonic crystal is realized in the near-infrared wavelengths. Comparing to a blackbody cavity radiation at $T\sim 1500$ K, its emission has a spectral width nearly 2.5 times narrower and also peaks at a lower wavelength of $\lambda\sim 1.5$ μm. Based on the spectral radiance, a proper length scaling and a planar TPV model calculation, a PBG emitter can yield an optical-to-electric conversion efficiency of $\sim 34\%$ and electrical power density of ~ 14 W/cm^2 at $\langle T\rangle\sim 1535$ K. A PBG emitter, thus, offers a potentially better efficiency and power over conventional emitters, including the blackbody cavity, the Er_2O_3, and the structured tungsten emitters.

The authors thank J. Gee for valuable discussion and J. Bur, M. Tuck, and J. Rivera for technical support. The work at Sandia National Laboratories is supported through DOE. Sandia is a multiprogram laboratory operated by Sandia Corporation, a Lockheed Martin Company, for the United States Department of Energy under Contract No. DE-AC04-94AL 85000.

[1] T. J. Coutts and M. C. Fitzgerald, Sci. Am. **1998**(7), 90.
[2] M. Zenker, A. Heinzel, G. Stollwerck, J. Ferber, and J. Luther, IEEE Trans Electron Devices **48**, 367 (2001).
[3] A. Heinzel, V. Boerner, A. Gombert, B. Blasi, V. Wittwer, and J. Luther, J. Mod. Opt. **47**, 2399 (2000).
[4] M. U. Pralle, N. Moelders, M. P. McNeal, I. Puscasu, A. C. Greenwald, J. T. Daly, E. A. Johnson, T. George, D. S. Choi, I. El-Kady, and R. Biswas, Appl. Phys. Lett. **81**, 4685 (2002).
[5] S. Y. Lin, J. G. Fleming, E. Chow, J. Bur, K. K. Choi, and A. Goldberg, Phys. Rev. B **62**, R2243 (2000).
[6] C. M. Cornelius and J. P. Dowling, Phys. Rev. A **59**, 4736 (1999).
[7] J. G. Fleming, S. Y. Lin, I. El-Kady, R. Biswas, and K. M. Ho, Nature (London) **417**, 52 (2002).
[8] S. Y. Lin, J. G. Fleming, I. El-Kady, and K. M. Ho (unpublished).
[9] J. D. Joannopoulos, R. D. Meade, and J. N. Winn: *Photonic Crystal* (Princeton University Press, Princeton, 1995).
[10] K. M. Ho, C. T. Chan, C. M. Soukoulis, R. Biswas, and M. Sigalas, Solid State Commun. **89**, 413 (1994).
[11] E. Ozbay, B. Temelkuran, M. M. Sigalas, G. Tuttle, C. M. Soukoulis, and K. M. Ho, Appl. Phys. Lett. **69**, 3797 (1996).
[12] M. A. Ordal, L. L. Long, R. J. Bell, S. E. Bell, R. R. Bell, R. W. Alexander, Jr., and C. A. Ward, Appl. Opt. **22**, 1099 (1983).
[13] S. Y. Lin, J. G. Fleming, Z. Y. Li, I. El-Kady, R. Biswas, and K. M. Ho, J. Opt. Soc. Am. B **20**, 1538 (2003).
[14] N. A. R. Bhat and J. E. Sipe, Phys. Rev. E **64**, 056604 (2001).
[15] K. Sakoda, *Optical Properties of Photonic Crystals* (Springer, New York, 2001), Chap. 5, p. 108.
[16] R. Loudon, *The Quantum Theory of Light* (Clarendon, Oxford, 1983), Chap. 1, pp. 13–17 and Chap. 5.
[17] S. Y. Lin, J. G. Fleming, D. L. Hetherington, B. K. Smith, R. Biswas, K. M. Ho, M. M. Sigalas, W. Zubrzycki, S. R. Kurtz, and J. Bur, Nature (London) **394**, 252 (1998).
[18] J. G. Fleming and S. Y. Lin, Opt. Lett. **24**, 49 (1999).